J. Min. Metall. Sect. B-Metall. 47 (1) B (2011) 11 - 21

Journal of Mining and Metallurgy

EFFECT OF RARE EARTH CE ON THE MICROSTRUCTURE, PHYSICAL PROPERTIES AND THERMAL STABILITY OF A NEW LEAD-FREE SOLDER

W. Chen, J. Kong# and W.J. Chen

Department of Materials Science and Engineering, Nanjing University of Science and Technology, Nanjing, P.R. China

(Received 28 August 2010; accepted 25 November 2010)

Abstract

In this paper, in order to develop a low silver content lead-free solder with good overall properties, a newly designed solder alloys of Sn-0.3Ag-0.7Cu-20Bi-xCe type, with addition of varying amounts of rare earth Ce (0.05 mass%, 0.1 mass% and 0.2 mass%) were studied. The melting temperature of Sn-0.3Ag-0.7Cu can be decreased substantially through addition of 20 mass% Bi; while the segregation of Bi element in the microstructure of the as-cast alloys can be relieved by micro-alloying with trace amount of rare earth Ce. Besides, aging treatments (160 °C held for 6 h) of these solder alloys imply that appropriate amount of Ce addition can not only depress the diffusion induced aggregation of Bi in the microstructure but promote the homogenization during annealing. Compared with Bi-free Sn-0.3Ag-0.7Cu solder, Sn-0.3Ag-0.7Cu-20Bi exhibits better wettability. More excitingly, the wetting property of Sn-0.3Ag-0.7Cu-20Bi can be further improved by doping little amounts of Ce, especially 0.5 mass%, in which case the spreading area of the solder can be increased to the largest extent. On the whole, the present study reveals that Sn-0.3Ag-0.7Cu-20Bi-xCe (x=0.05-0.1) is a promising lead-free solder candidate considering the microstructure, melting temperature and wetting properties.

Keywords: lead-free solders; rare earth Ce; microstructure; physical properties; thermal stability; aging treatment.

1. Introduction

With the urgent requirement for a Pb-free environment, extensive efforts have been made in developing many lead-free solder systems to be utilized in electronics industry,

Corresponding author: kongjian68@163.com

DOI:10.2298/JMMB1101011C

such as Sn-Cu, Sn-Zn, Sn-Ag, Sn-Bi, Sn-Ag-Cu, Sn-Zn-Bi and so forth [1-5]. Although various alloy systems have been identified as potential candidates to substitute the traditional Sn-Pb solder, none of them satisfy all the criteria regarding temperature compatibility (close melting temperature to Sn-Pb solder), good wettability, excellent mechanical reliability as well as low material cost [6, 7]. Among all lead-free solder candidates, low silver content ternary alloy Sn-0.3Ag-0.7Cu has been widely studied because of its remarkably lower cost and superior solderability [8-11], but its high melting temperature and unsatisfactory wetting property hinder the wider application. While Sn-Bi solders possess merits of low cost, sufficiently low melting point and good wettability, their defects lie in the weak mechanical properties and inferior solderability originating from the concentration of Bi element or dendritic segregation in the microstructure of the solder alloys and the ultimate solder joints [12-14]. In the present work, aiming to find a low silver content lead-free solder with outstanding global properties, a new Sn-0.3Ag-0.7Cu-20Bi solder alloy with prominent wetting property, low melting temperature as well as favorable microstructure has been designed.

Previous studies showed that rare earths could be considered as active "vitamin"-metals and be used for microstructural refinement, thus making a great improvement in the whole performance of lead-free solders [7, 15-19]. In this research, to overcome the vital problem of Bi-segregation in the new solder microstructure, the effects of varying amounts of Ce addition ranging from 0.05 mass% to 0.2 mass% on the microstructure and physical properties of the solder alloy Sn-0.3Ag-0.7Cu-20Bi have also been investigated. In addition, it is well known that electronic devices nowadays are not only utilized in normal working environments but occasionally subjected to higher temperatures as well [5, 20, 21], which demands excellent thermal fatigue resistance for lead-free solders. Unfortunately, Bi containing lead-free solders often suffer from thermal failure owing to the microstructure instability at high temperatures [22-24]. Accordingly, thermal aging has been carried out in the present investigation to simulate the microstructure evolution of all prepared solder alloys at high temperatures, which can also assist in understanding the effect of rare earth Ce on the microstructural stability.

2. Experimental

The pure metals Sn (99.9 mass%), Ag (99.99 mass%), Cu (99.99 mass%), Bi (99.95 mass%) and rare earth Ce (99.99 mass%) were used as raw materials. Firstly, Sn, Ag, Cu, Bi were mixed and melted in a Al_2O_3 ceramic crucible at 853 K for approximately 40 min in a chamber-type electric resistance furnace (SX_5-5-11Q). Because of the reactive nature with oxygen, the rare earth Ce was mixtured into the molten alloy Sn-Ag-Cu-Bi using a cast-iron bell with holes on the sidewall. After Ce was melted, the alloy Sn-Ag-Cu-Bi-Ce was maintained for another 60 min, during which mechanical stirring was performed every 10 min through a glass rod, to assure the homogenization of the solder alloy. In the

whole process of melting, it should be noted that a dose of eutectic salt of KCl and LiCl with the mass ratio of 1.3:1 (KCl:LiCl = 1.3:1) was employed to protect the surface of the metal liquid against oxidation by the atmospheric air. Eventually, the molten alloy was casted into a rod ingot with a diameter of 12 mm. In order to display the disparities of the presently designed solder alloy Sn-0.3Ag-0.7Cu-20Bi-xCe (x=0, 0.05, 0.1, 0.2) with the previously studied Sn-0.3Ag-0.7Cu, the latter Sn-0.3Ag-0.7Cu alloy ingots were prepared as well. The nominal chemical compositions of all samples are listed in Table I. The aging treatment of each as-cast ingot was carried out in a resistance oven at 160 ^{o}C ±5 ^{o}C held for 6 h.

The microstructure of the as-cast and aging treated alloys was observed using an Olympus BX60M optical microscopy (OM). An agent of 20 mL HCl plus 100 mL H_2O mixed with 10 g $FeCl_3$ was prepared to etch each alloy for about 10 s. Some areas were enlarged for careful observation using scanning electron microscopy (SEM, JEOL Model JSM-6490) equiped with energy-dispersive X-ray spectroscopy (EDX).

The melting temperature of various solder piece samples with a mass of 10 mg (±1 mg) were determined by the STA449C6 differential scanning calorimetry (DSC). All samples were measured at a constant heating rate of 6 K/min from 303 K to 573 K in a flowing argon atmosphere.

Solder wettability experiments were evaluated with respect to the spreading area of a certain mass amount 0.2 g (±1%) of small solder balls conducted in the electric resistance furnace. Commercial copper pads (40 mm × 40 mm × 3 mm) were employed as substrates in the wetting tests. Before testing, the solder spheres were completely cleaned in acetone for about 5 min and the copper pads were polished with 1200# abrasive papers to ensure better surface smoothness. The wettability tests were performed at 270 ^{o}C for 240 s. It is worth noting that prior to the tests, the solder spheres and the touched copper substrates were covered by approximately 0.1 g activated flux of rosin in order to prevent oxidation. Afterwards, the solder joints were taken out for air cooling. To calculate the average spreading area of the three samples for each composition, the spreading samples were all scanned in into a computer and the areas were obtained by software. Three measurements were performed for each solder composition and an average value was adopted. In addition, the wettability measurements were also conducted on a typical commercial Sn-37Pb solder for reference.

Table I. Chemical compositions of specimens.

Alloy	Sn (wt%)	Ag (wt%)	Cu (wt%)	Bi (wt%)	Ce (wt%)	Pb (wt%)
Sn-0.3Ag-0.7Cu	99	0.3	0.7	/	/	/
Sn-0.3Ag-0.7Cu-20Bi	79	0.3	0.7	20	/	/
Sn-0.3Ag-0.7Cu-20Bi-0.05Ce	78.95	0.3	0.7	20	0.05	/
Sn-0.3Ag-0.7Cu-20Bi-0.1Ce	78.9	0.3	0.7	20	0.1	/
Sn-0.3Ag-0.7Cu-20Bi-0.2Ce	78.8	0.3	0.7	20	0.2	/

3. Results and Discussions

3.1 Microstructure of as-cast alloys

Fig. 1 shows the optical micrography photographs of all as-cast samples in this work. It can be seen from Fig. 1 (a) that the microstructure of as-cast Sn-0.3Ag-0.7Cu ternary alloy consists of β-Sn matrix, gray pro-eutectic phase β-Sn and some tiny bright phases distributed between these two phases, which is nearly in consistent with available study on this alloy reported by Kanlayasiri *et al* [8]. These tiny bright phases should be Sn-Ag-Cu eutectics, postulated to be a mixture of two intermetallics - Ag_3Sn and Cu_6Sn_5, distributed in β-Sn matrix. With the addition of 20 mass% Bi element, it can be clearly found that aside from the phases described above, many isolated white needle-like precipitates appear out of the matrix [shown in Fig. 1 (b)]. To clarify this phase, EDX was employed to investigate the elemental distribution of the domain around the needle-like phase as shown in Fig. 2. It is noted that Sn, Ag, and Cu elements are almost distributed homogeneously and the needle-shaped substances are all Bi-rich phase checked by EDX. This phenomenon of segregation of Bi element is a common feature in many high Bi-bearing lead-free solders as was proved elsewhere [12, 25, 26]. In this study, since the amounts of Ag and Cu are limited, the concentration of Bi should not arise from Sn consumption by formation of intermetallic compounds Ag_3Sn and Cu_6Sn_5. Instead, it ought to stem from the solidification segregation. It was reported that solubility of Bi element in Sn is merely approximately 1 mass% at room temperature, which seems to be in line with the Bi segregation in this study [22, 27]. Fortunately, from Fig. 1 (c), (d), and (e), it is unambiguous that by adding small amounts

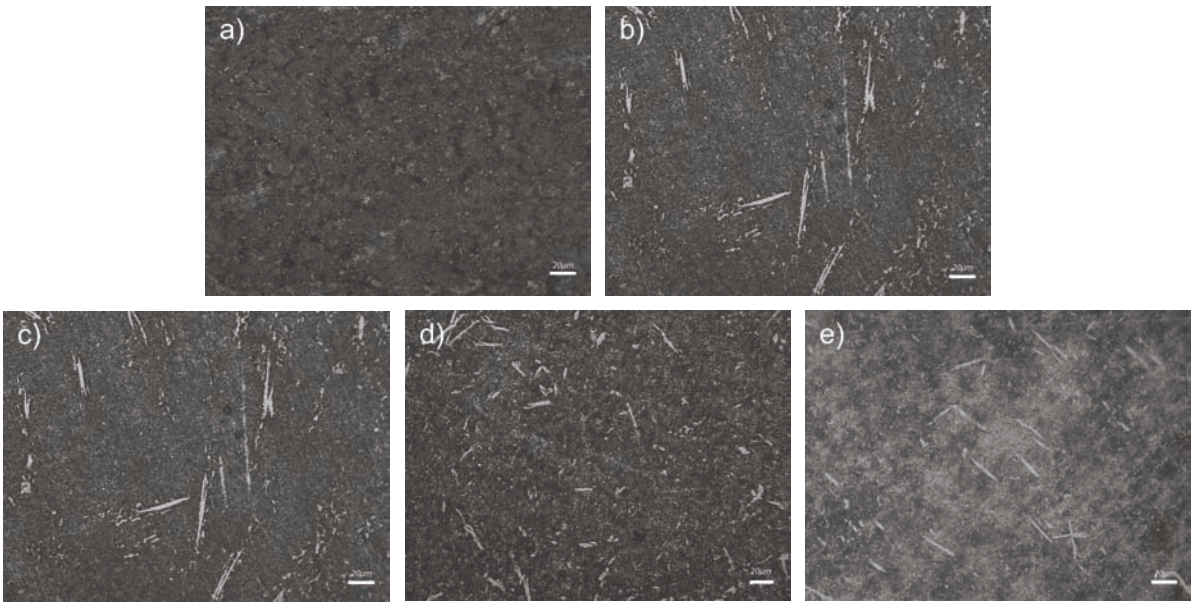

Fig. 1 Microstructure of as-cast alloys, a) Sn-0.3Ag-0.7Cu; b) Sn-0.3Ag-0.7Cu-20Bi; c) Sn-0.3Ag-0.7Cu-20Bi-0.05Ce; d) Sn-0.3Ag-0.7Cu-20Bi-0.1Ce; e) Sn-0.3Ag-0.7Cu-20Bi-0.2Ce.

of rare earth Ce, the segregation of Bi is remarkably impaired. Furthermore, among three attempts of different contents of Ce addition, this segregation alleviating effect is achieved to the largest extent when the proportion of Ce is about 0.05 mass%. With further increment of rare earth Ce, this modification effect of Bi concentration goes toward deterioration. In fact, Bi-rich phases are generally quite brittle in nature, which can lead to more inferior mechanical properties for the solder, and even result in the disappointing "peeling off" phenomenon for the ultimate solder joints [13, 28-30]. Additionally, careful investigation of the microstructure of all these alloys indicates that the rare earth Ce can not only refine the Bi-rich precipitates, but also refine the entire microstructure in all three different doping cases. This refinement of microstructure can be attributed to the intrinsic characteristics of Ce atoms. In general, Ce is extraordinarily close to Sn and this can promote the formation of Sn-Ce compounds having high melting point in grain boundaries [31]. Alternatively, the atomic radius of Ce is far larger than that of others in the alloy and the remaining Ce atoms are liable to gather or be absorbed by the grain boundaries. These Ce atoms tend to affect the diffusion of Sn atoms and behave as a barrier to defer the growth velocities of intermetallic compounds Ag_3Sn and Cu_6Sn, subsequently [7, 32]. In either case, the remaining Ce atoms or Sn-Ce compounds can act as inhomogeneous center of nucleation and afterwards degrade the growth velocities of intermetallics, thus inducing the intermetallics more uniformly distributed and the microstructure much finer.

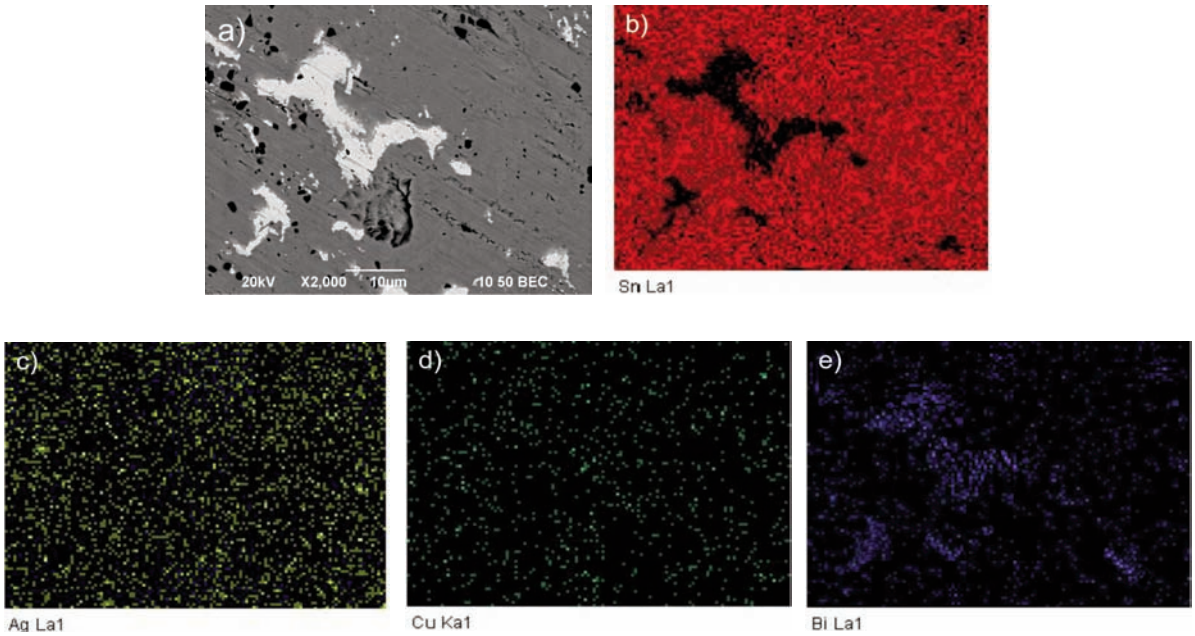

Fig. 2 Elemental distribution in Sn-0.3Ag-0.7Cu-20Bi characterized by X-ray mapping, a) microstructure of Sn-0.3Ag-0.7Cu-20Bi; b) Sn mapping graph; c) Ag mapping graph; d) Cu mapping graph; e) Bi mapping graph.

3.2 Thermal analysis and melting properties

Fig. 3 shows the DSC curves of all tested samples. The melting charateristics are summarized in Table II. The solidus point, T_s, and liquidus point, T_l, are both determined through double tangent method. Compared with the melting temperature (183 ^oC) for Sn-Pb solder, all Bi bearing solders in this work have extremely close onset melting temperature (T_s), which is of essential significance in soldering technology. In this sense, it should be noticed that the melting temperature of Sn-0.3Ag-0.7Cu can be decreased tremendously by adding 20 mass% Bi. It is known that the melting point of Bi itself is quite low and deriving from the binary phase diagram, Bi can not combine with Sn to form high melting temperature intermetallics. Moreover, the Sn-Bi solid solution also possesses a low liquidus temperature when the Bi content reaches up to 20 mass%. However, the addition of Bi element can expand the pasty range of the solder from 5.2 ^oC to 14 ^oC, which may be due to the hyper-eutectic formation accompanied by Bi alloying. After adding Ce into the solder, slight increases in T_s,T_l,T_p, and pasty range ΔT are detected. Nevertheless, the melting properties nearly keep steady and change negligibly when varying the amount of rare earth Ce addition. In particular, it is worthy to mention that an exothermic peak appears at the temperature range of 140 ^oC~150 ^oC, followed by a tiny endothermic peak (shown by the arrow) at around 140 ^oC in DSC curves of all Bi bearing solder alloys. Suppose that some Sn-Bi eutectics are highly possible to nucleate and grow rapidly at the final stage of non-equilibrium solidification, the melting process of Sn-Bi eutectic at its melting point 139 ^oC upon heating should be responsible

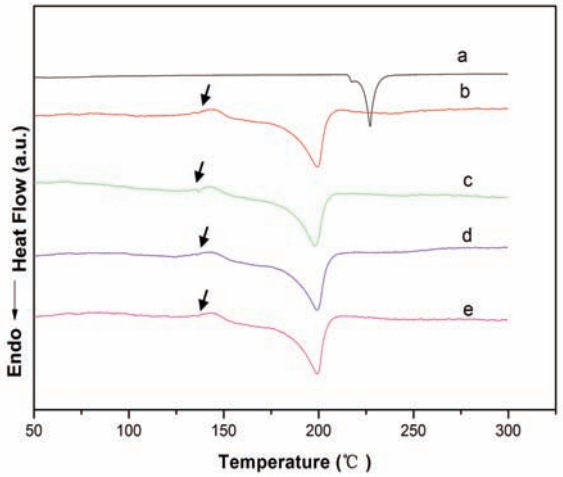

Fig. 3 DSC curves of all tested samples, a) Sn-0.3Ag-0.7Cu; b) Sn-0.3Ag-0.7Cu-20Bi; c) Sn-0.3Ag-0.7Cu-20Bi-0.05Ce; d) Sn-0.3Ag-0.7Cu-20Bi-0.1Ce; e) Sn-0.3Ag-0.7Cu-20Bi-0.2Ce.

Table II. The meltingl properties for all the tested specimens.

Alloy composition	Solidus temperature T_s (^oC)	Liquidus temperature T_l (^oC)	Peak temperature T_p (^oC)	Pasty range DT (^oC)
Sn-0.3Ag-0.7Cu	225.8	231	227.1	5.2
Sn-0.3Ag-0.7Cu-20Bi	184.9	204.1	198.9	14
Sn-0.3Ag-0.7Cu-20Bi-0.05Ce	187	198.4	202	15
Sn-0.3Ag-0.7Cu-20Bi-0.1Ce	187	199.4	202.8	15.8
Sn-0.3Ag-0.7Cu-20Bi-0.2Ce	188.4	199.2	203.5	15.1

for this tiny endothermic peak. Afterwards, it is reasonable to deduce that this eutectic dissolution into the matrix is bound to be characterized by amounts of heat release, corresponding to the ensuing exothermic peak. In this light, it can evidently explain the adverse consequence of Bi agglomeration in many Bi-containing lead-free solder working at high temperatures since the non-equilibrium solidification elicited Sn-Bi eutectic dissolution could enhance the possibility of the attachment of dissolved Bi to existing Bi-rich phases in the microstructure.

3.3 Wetting properties

The spreading areas of all tested alloys in this study as well as the commercial Sn-Pb solder were measured and listed in Table III. From this table, it is obvious that addition of 20 mass% Bi into Sn-0.3Ag-0.7Cu can improve its spreading area by around 11%. This can be analyzed from the following three perspectives. For one thing, Sn and Bi elements can hardly form high melting temperature intermetallics and Bi atoms can not affect the spreading behaviour of original Sn-0.3Ag-0.7Cu alloy on the Cu plate. For another, in comparison with Sn-0.3Ag-0.7Cu alloy, the Bi containing Sn-0.3Ag-0.7C-20Bi displays a much lower melting temperature, which inclines to produce a much higher degree of "superheating" effect during melting and spreading at 270 ^{o}C, thus yielding a larger spreading area. The most important is that Bi can be taken as a surface-active element that can reduce the surface tension of the solder alloy substantially. According to Young's equation, a smaller contact angle will follow a smaller surface tension, thereby seeding the origin of a larger spreading area. More interestingly, the spreading area of Sn-0.3Ag-0.7C-20Bi-0.05Ce is even larger than that of Sn-0.3Ag-0.7C-20Bi, reaching a maximum value of 52.9 mm^2, i.e., a comparative value of 80.6% relative to Sn-Pb solder. But this ameliorative effect in wettability goes downward with further increasing the content of Ce to 0.1 mass% or 0.2 mass%. In any way, all three Ce containing alloys exhibit better wettability than Sn-0.3Ag-0.7Cu alloy. It has been recognized that Ce is also a kind of surface-active element, called "vitamin" of metals. A proper addition of it can lower down the interfacial surface tension between the

Table III. Spreading areas of the lead-free solders in this study and the commercial Sn-Pb solder as reference.

Composition	Spreading area (mm^2)	Comparative spreading area (take the spreading area of Sn-Pb alloy as 100%)
Sn-0.3Ag-0.7Cu	39	59.50%
Sn-0.3Ag-0.7Cu-20Bi	43.4	66.20%
Sn-0.3Ag-0.7Cu-20Bi-0.05Ce	52.9	80.60%
Sn-0.3Ag-0.7Cu-20Bi-0.1Ce	49	74.70%
Sn-0.3Ag-0.7Cu-20Bi-0.2Ce	45.1	68.80%
Commercial Sn-Pb alloy	65.6	100%

molten solder and Cu substrate and render a more superior flowable liquid solder [17, 33]. Hence, the wettability should be enhanced in this regard. Furthermore, rare earth Ce is quite chemically active in nature and it can react with the atmospheric oxygen. This undoubtedly reduce the opportunity of the reaction between Cu substrate and oxygen, making the oxide layer product less possible. In other words, the resistance of interfacial reaction between Cu substrate and molten solder alloy can be impaired considerably, which helps to creat a more favorable condition for spreading. However, excessive amount of Ce could induce the formation of Ce-containing compounds. These compounds often precipitate on the surface of Cu substrate and hamper the spreading process of the solder [34]. So, it is understandable that an appropriate controll of Ce addition plays a critical role in the enhancement of wettability for lead-free solders.

3.4 Microstructure after aging treatment

As mentioned above, Bi bearing lead-free solders usually suffer from thermal failure due to their microstructure instability, especially the Sn-Bi eutectic dissolution at temperature higher than 139 ^{o}C. As qualified lead-free solder candidates, they should own good thermal stability at high temperatures. Therefore, it is necessary for the present work to investigate the thermal stability of the microstructure of all the alloys after thermal aging treatment at a temperature higher than this sensitive temperature.

Fig. 4 shows the microstructure of all tested solder alloys after thermal aging treatment. It can be seen from Fig. 4(a) that there seems no apparent alternation in Sn-0.3Ag-0.7Cu alloy except for a slight increase in the size of gray β-Sn phase. Fig. 4(b), (c), (d), (e) reveal that in the alloys Sn-0.3Ag-0.7Cu-20Bi and Sn-0.3Ag-0.7Cu-

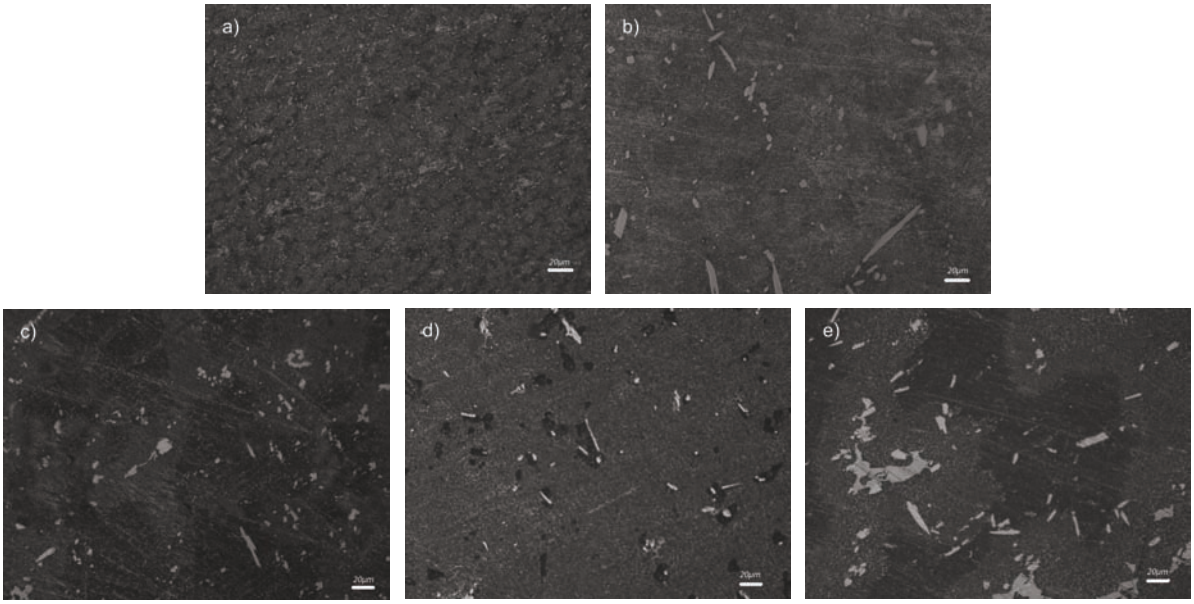

Fig. 4 Microstructure of thermal aging treated alloys, a) Sn-0.3Ag-0.7Cu; b) Sn-0.3Ag-0.7Cu-20Bi; c) Sn-0.3Ag-0.7Cu-20Bi-0.05Ce; d) Sn-0.3Ag-0.7Cu-20Bi-0.1Ce; e) Sn-0.3Ag-0.7Cu-20Bi-0.2Ce.

20Bi-0.2Ce, much more severe congregation of Bi element took place after aging treatment in contrast with their microstructure under as-cast state. This severe consequence, however, is not discovered in the Sn-0.3Ag-0.7Cu-20Bi-0.05Ce solder alloy. More surprisingly, for the solder Sn-0.3Ag-0.7Cu-20Bi-0.1Ce, the originally vicious segregation of Bi in the as-cast alloy can even be eliminated to some extent. In other words, appropriate amount of Ce can refine the Bi-rich phase for this alloy upon aging treatment. Theoretically, three possible detrimental processes may occur accompanied by aging. One is the dissolution of Sn-Bi eutectic at the final stage of non-equilibrium solidification into the matrix, followed by the attachment of the dissolved Bi to existing Bi-rich phases to form larger bulks as discussed before. Secondly, aging induced precipitation of oversaturated Bi during non-equilibrium solidification process out of the Sn matrix may occur. These precipitated Bi can also attach to the existing Bi-rich phases or congregate together, growing to coarser bulks with the help of thermally driven diffusion. Meanwhile, the Ostwald ripening tends to happen probably by means of Bi diffusion, which is able to result in the consequence that big Bi particles grow bigger at the cost of the small ones go smaller or vanished. Thirdly, an advantageous consequence, i.e., homogenization process evoked by diffusion annealing cannot be ignored during isothermal treatment. After all, the diffusion ability of atoms at 160 ^{o}C should be much stronger than at room temperature. Thereby, the precipitation of Bi from the matrix and the diffusion homogenization ought to co-exist during thermal aging. As for the two alloys Sn-0.3Ag-0.7Cu-20Bi and Sn-0.3Ag-0.7Cu-20Bi-0.2Ce, the congregation of Bi seems to play a more dominant role. Yet, in the Sn-0.3Ag-0.7Cu-20Bi-0.05Ce and Sn-0.3Ag-0.7Cu-20Bi-0.1Ce alloys, the long-range diffusion of Bi into the matrix prevails, which can weaken the concentration of Bi and engender the dissipation or thinning of some needle-shaped Bi. In fact, the congregation of Bi can be regarded as a sort of uphill diffusion while the thinning of Bi can be deemed as a downhill diffusion. The driven force for these two types of diffusion both result from the chemical potential divergence of the Bi-containing phases within the microstructure. From this perspective, it is reasonable to speculate that different amounts of Ce addition may lead to different transformations in chemical potential configuration of those Bi-containing phases. Excessive amount of Ce addition can bring about adverse effect. In the cases that 0.5 mass% and 0.1 mass% Ce addition into Sn-0.3Ag-0.7Cu-20Bi can achieve exciting effects in suppressing the coarsening of Bi and refining the microstructure at a high temperature, it is supposed that this is mainly attributable to the deferring effect of the three processes discussed above. Given the long time scale and high temperature for the aging treatment in this study, the most important effect of rare earth Ce is assumed to lie in retarding the Ostwald ripening process [35], although the real underlying mechanisms involved need to be further studied in future. From the results of this present study, it is clear that a diffusion annealing procedure can be applied

for the alloys Sn-0.3Ag-0.7Cu-20Bi-0.05Ce and Sn-0.3Ag-0.7Cu-20Bi-0.1Ce during solder production to further decrease the degree of Bi concentration, if available. However, the temperature for diffusion annealing must be controlled not overhigh to avoid the appearance of liquid phase; otherwise, superburning of the alloy could arise.

4. Conclusions

20 mass% Bi was added into Sn-0.3Ag-0.7Cu solder alloy to reduce the melting temperature and improve the wetting property of the solder, and the Bi segregation in the microstructure can be greatly alleviated by microalloying of rare earth Ce. Apart from refinement of the microstructure of the alloy, Ce can also enhance the wetting property of the solder alloy Sn-0.3Ag-0.7Cu-20Bi, and achieve a best ameliorative effect in microstructure and wetting property when the adding amount is governed as 0.05 mass% in this work. Aging treatment at 160 ^{o}C for 6 h shows that adding appropriate amount of Ce into Sn-0.3Ag-0.7Cu-20Bi can breed more stable microstructure to prevent serious Bi concentration; while Ce-free Sn-0.3Ag-0.7Cu-20Bi and Sn-0.3Ag-0.7Cu-20Bi-0.2Ce containing excessive Ce, both have a serious problem of Bi congregation at a high temperature, resulting in poor thermal stability of microstructure. To conclude, taking a combined consideration of low materials cost, as-cast microstructure, melting temperature, wettability as well as thermal stability of microstructure, which is an essential concern for lead-free solders being utilized under thermal exposure environment, the low silver content alloy Sn-0.3Ag-0.7Cu-20Bi-xCe (x=0.05-0.1) is believed to be an encouraging candidate as a substitute of Sn-Pb solder.

Acknowledgements

The works is supported by Natural Science Foundation of Jiangsu Province of China (BK2006206, kjsmcx06002), and Young Scholar Foundation of Nanjing University of Science and Technology (AB41325). It is highly grateful to H.H. Zhou for the experimental assistance.

References:

[1] H.W. Miao, J.G. Duh, Materials Chemistry and Physics 71 (2001) 255.

[2] S.-H. Huh, K.-S. Kim, K. Suganuma, Materials Transactions 42 (2001) 739.

[3] J.-E. Lee, K.-S. Kim, M. Inoue, J.X. Jiang, K. Suganuma, Journal of Alloys and Compounds 454 (2008) 310.

[4] V. Gandova, K. Lilova, H. Malakova, B. Huber, N. Milcheva, H. Ipser, J. Vrestal, G. Vassilev, Journal of Mining and Metallurgy Section B-Metallurgy 46 (1) B (2010) 11.

[5] H. Ipser, Journal of Mining and Metallurgy Section B-Metallurgy 43 (2) B (2007) 109.

[6] A. Kroupa, A.T. Dinsdale, A. Watson, J. Vrestal, A. Zemanova, Journal of Mining and Metallurgy Section B-Metallurgy 43 (2) B (2007) 113.

[7] C.M.L. Wu, D.Q. Yu, C.M.T. Law, L. Wang, Materials Science and Engineering: R 44 (2004) 1.

[8] K. Kanlayasiri, M. Mongkolwongrojn, T. Ariga, Journal of Alloys and Compounds 485 (2009) 225.

[9] I.G.B.B. Dharma, M.H.A. Shukor, T. Ariga, Materials Transactions 50 (2009) 1135.

[10] K.-S. Kim, S.H. Huh, K. Suganuma, Journal of Alloys and Compounds 532 (2003) 226.

[11] F. San, P. Hochstenbach, W.D. Van Driel, G.Q. Zhang, Microelectronics Reliability 48 (2008) 1167.

[12] H. Takao, H. Hasegawa, Journal of Electronic Materials 30 (2001) 513.

[13] K. Suganuma, Scripta Materialia 138 (1998) 1333.

[14] K. Suganuma, Technology of lead-free soldering. Beijing. Science Press, 2004, pp. 51.

[15] A. Ramirez, H. Mavoori, S. Jin, Applied Physics Letters 80 (2002) 398.

[16] Y. Yu, Z.D. Xia, F. Guo, Y.W. Shi, Journal of Electronic Materials 37 (2008) 975.

[17] D.Q. Yu, J. Zhao, L. Wang, Journal of Alloys and Compounds 376 (2004) 170.

[18] L. Zhang, S.B. Xue, L.L. Gao, G.Zeng, Y. Chen, S.L. Yu, Z. Sheng, Transactions of Nonferrous Metals Society of China 20 (2010) 412.

[19] X.Y. Zhao, M.Q. Zhao, X.Q. Cui, T.H. Xu, M.X. Tong, Transactions of Nonferrous Metals Society of China 17 (2007) 805.

[20] D. Živković, D. Minić, D. Manasijević, A. Kostov, N. Talijan, Lj. Balanović, A. Mitovski, Ž. Živković, Journal of Mining and Metallurgy Section B-Metallurgy 46 (1) B (2010) 105.

[21] S. Marjanović, D.Gusković, M. Trucić, B. Marjanović, Journal of Mining and Metallurgy Section B-Metallurgy 43 (2) B (2007) 177.

[22] J. Zhao, L.Qi, X.M. Wang, L. Wang, Journal of Alloys and Compounds 375 (2004) 196.

[23] Y. Kariya, Y. Hirata, M. Otsuka, Journal of Electronic Materials 28 (1999) 1263.

[24] N.M. Poon, C.M.L. Wu, J.K.L. Lai, Y.C. Chan, IEEE Transactions on Advanced Packaging 23 (2000) 708.

[25] F. Rosalbino, E. Angelini, G. Zanicchi, R. Marazza, Materials Chemistry and Physics 109 (2008) 386.

[26] C.W. Hwang, K. Suganuma, Materials Science and Engineering: A 373 (2004) 187.

[27] B.T.K. Barry, C.J. Thwaites, Tin and its alloys and compounds. England: Ellis Horwood Limited, John Wiley & Sons, 1983, p. 37.

[28] C.M. Chuang, T.S. Lui, L.H. Chen, Journal of Materials Science 37 (2002) 191.

[29] S. Sengupta, H. Soda, A. McLean, Journal of Materials Science 37 (2002) 1747.

[30] H. Ohtani, K. Ishida, Journal of Electronic Materials 23 (1994) 747.

[31] M.A. Dudek, N. Chawla, Nanoindentation of rare earth-Sn intermetallics in Pb-free solders, Intermetallics., 18 (5) (2010) 1016.

[32] Z.D. Xia, Journal of Materials Science 31 (2002) 564.

[33] Z.G. Chen, Y.W. Shi, Z.D. Xia, Y.F. Yan, Journal of Electronic Materials 32 (2003) 235.

[34] Y.W. Shi , J. Tian, Journal of Alloys and Compounds 453 (2008) 180.

[35] H. Hao, Y.W. Shi, Z.D. Xia, Y.P. Lei, F. Guo, Journal of Electronic Materials 37 (2008) 2..